Nonlinear actuation of micromechanical Casimir oscillators with topological insulator materials toward chaotic motion

Tajik, F; Allameh, N; Masoudi, A A; Palasantzas, G

Published in:
Chaos

DOI:
10.1063/5.0100542

Publication date:
2022

Chaos

Nonlinear actuation of micromechanical Casimir oscillators with topological insulator materials toward chaotic motion: Sensitivity on magnetization and dielectric properties

Cite as: Chaos **32**, 093149 (2022); https://doi.org/10.1063/5.0100542
Submitted: 25 May 2022 • Accepted: 26 August 2022 • Published Online: 30 September 2022

F. Tajik, N. Allameh, A. A. Masoudi, et al.

Nonlinear actuation of micromechanical Casimir oscillators with topological insulator materials toward chaotic motion: Sensitivity on magnetization and dielectric properties

Cite as: Chaos **32**, 093149 (2022); doi: 10.1063/5.0100542
Submitted: 25 May 2022 · Accepted: 26 August 2022 ·
Published Online: 30 September 2022

F. Tajik,[1,2] N. Allameh,[1] A. A. Masoudi,[1] and G. Palasantzas[2,a)]

AFFILIATIONS

[1] Department of Physics, Faculty of Physics and Chemistry, Alzahra University, Tehran 1993891167, Iran
[2] Zernike Institute for Advanced Materials, University of Groningen, Nijenborgh 4, 9747 AG Groningen, The Netherlands

[a)] **Author to whom correspondence should be addressed:** g.palasantzas@rug.nl

ABSTRACT

We have investigated the dynamical actuation of micro-electromechanical systems under the influence of attractive and repulsive Casimir forces between topological insulator plates as a function of their dielectric function and coating magnetization. The analysis of the Casimir force in the limit of strong and weak magnetization shows that the attractive force, which is produced for plate magnetizations in the same direction, is greater than the repulsive force that is produced for opposite magnetizations. However, both forces remain comparable for intermediate magnetizations. Moreover, for weak magnetization, the attractive force becomes stronger for an increasing dielectric function, while the opposite occurs for the repulsive force. On the other hand, increasing magnetization decreases the influence of the dielectric function on both the repulsive and attractive forces. Furthermore, for conservative systems, bifurcation and phase portrait analysis revealed that increasing magnetization decreases the regime of stable operation for devices with attractive forces, while their operation remains always stable under the presence of repulsive forces. Finally, for non-conservative periodically driven systems, the Melnikov function and Poincaré portrait analysis show that for magnetizations in the same direction leading to strong attractive Casimir forces, chaotic motion toward stiction is highly likely to occur preventing the long-term prediction of actuating dynamics. A remedy for this situation is obtained by the application of any magnetization in opposite directions between the interacting surfaces since the repulsive force makes it possible to prevent stiction.

Nowadays, from both fundamental science and technology points of view, the attention on surface interactions in micro/nanoelectromechanical systems is growing. Consequently, the omnipresent Casimir forces, mediated by quantum vacuum fluctuations, become inevitably important during device actuation. For devices with topological insulator components, the application of magnetization makes it feasible to change both the magnitude and sign of the Casimir force under certain conditions. Hence, our findings reveal strong sensitivity between device actuation and applied magnetization because the achievement of repulsive forces leads to devices that remain stable always. On the other hand, by increasing the magnitude of the magnetization in the same direction leading to attractive forces, the regime of stable operation decreases leading also to the chaotic motion toward stiction.

I. INTRODUCTION

The Casimir force, which was discovered by Casimir in 1948[1] between two parallel neutral plates, originates from the perturbation of quantum fluctuations of the electromagnetic field. Making boundaries at the micrometer and submicrometer scales leads to modification in the zero-point energy of the electromagnetic field by generating forces that cover both van der Waals (short range) and Casimir (long range where retardation is important) asymptotic regimes.[2–8] Later in the 1950s, Lifshitz and co-workers investigated the magnitude and action of the Casimir force for the general case of dielectric bodies.[6] The Lifshitz theory can be important in the development of microdevice technology because it allows us to tune the Casimir force using suitable materials.[9–14] In fact, over the last decades, there has been a growing demand for

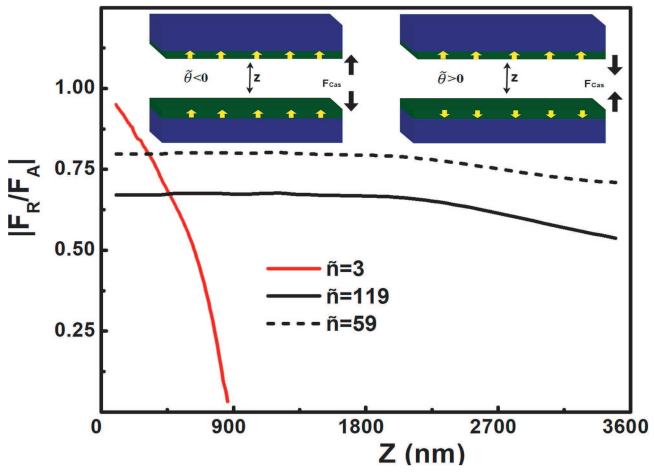

FIG. 1. The ratio of the repulsive to the attractive Casimir force (F_R/F_A) vs distance between plates using weak, intermediate, and strong magnetizations. The inset shows the schematic of the interacting topological insulator plates at a distance d ($<1\mu$m) being covered by a thin magnetic layer. Positive and negative values of $\tilde{\theta}$ ($= \theta_1\ \theta_2$) lead to attractive and repulsive Casimir forces, respectively.

micro-electromechanical devices (MEMSs) in a variety of technology applications and fundamental science. On the other hand, recent developments in novel materials have stimulated the advancement of microfabrication technologies and microdevice architectures. Because of the large surface area to distance ratio between MEMS components, the omnipresent Casimir force could have a major impact on the performance of these devices when they are scaled down to nanometer sizes.[3,15,16]

Moreover, the Casimir force is highly dependent on the geometry of devices,[14] and it is often attractive between two plates in vacuum.[1] Furthermore, due to the existence of attractive electrostatic and Casimir forces, which are commonly used to actuate microdevices, there is an inevitable instability known as stiction, which causes permanent adhesion between the components.[15,16] Hence, the development of pathways to reduce the stiction instability is of high importance, and because of their ability to generate repulsive Casimir forces under certain conditions, the use of topological insulator (TI) materials[17–21] in the architecture of MEMS is a promising proposal.[20–24]

Because of the magnetoelectric effect and its impact on the Maxwell equations and Fresnel coefficients, the Casimir force changes not only in magnitude but also in the direction.[20–24] At short separations, several studies have shown how the opposite direction of magnetization between two topological insulator plates can lead to repulsive Casimir forces.[17,21] However, so far, it remains unknown if a certain magnitude of the magnetization applied to the surface of the plates in both same and opposite directions will produce equally strong attractive and repulsive Casimir forces and more important will be its effect on the dynamical actuation of MEMS. Moreover, it is important to know if the ratio between the attractive and repulsive Casimir forces can remain constant over a large range of magnetization for device applications. Finally, how sensitive are

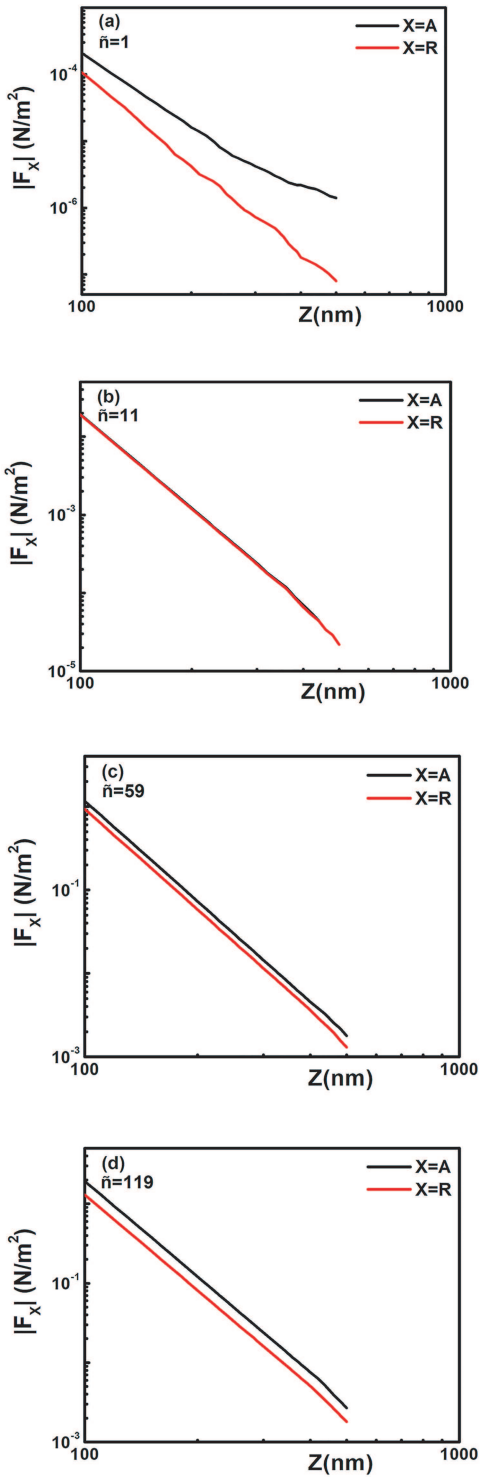

FIG. 2. Magnitude of the attractive and repulsive Casimir force F_A and F_R, respectively, vs the distance between plates using different magnetizations: (a) weak, (b) intermediate, (c) and (d) strong values.

the repulsive and attractive forces and consequently, the stable operation of devices to the dielectric function, and how this sensitivity can vary with the magnitude of the magnetization are points of direct concern for systems when TI materials are employed in device architectures. Therefore, the present study can provide important information for device manufacturing using novel materials. This is because despite the existence of other strong attractive forces, as, for example, electrostatic, the TI materials could offer a significant possibility against the chaotic motion and consequently, stiction due to the presence of repulsive Casimir forces.

II. MODEL AND METHOD

A. Casimir force calculation

Here, we have considered two parallel TI plates, which are covered by a thin magnetic layer [Fig. 1(a)]. The separation between the plates is considered to be less than 1 μm, and the effect of temperature is neglected by assuming T = 0 K. Using the Lifshitz theory, the Casimir energy between two parallel plates at T = 0 K is given by[4]

$$E(z) = \frac{\hbar}{4\pi^2}\int_0^\infty d\xi \int_0^\infty dk_\perp k_\perp \log\det[1 - R_1R_2\exp(-2k_0z)]. \quad (1)$$

In Eq. (1), ξ is the imaginary frequency ($\omega = i\xi$), $k_\perp$ is the in-plane wave vector, and $k_i = \sqrt{\varepsilon_i(i\xi_l)\xi^2/c^2 + k_\perp^2}$ with (i = 0, 1, 2) representing the out-off plane wave vector in the gap between the interacting plates. $R_{1,2}$ are the reflection matrices defined by Fresnel coefficients for the first and second plates, respectively. The Fresnel reflection coefficients are shown by r_s, $r_{p,}$ and r_{sp}, which describe the transverse electric mode (TE), transverse magnetic mode (TM), and mix polarizations (TEM), respectively. The reflection matrix contains r_s and r_p as the diagonal terms, and r_{sp} as the non-diagonal term (see the Appendix). The reflection matrices of a trivial TI plate (without a magnetic layer) are diagonal, while the magnetic layer on the TI plates (referred to as non-trivial TI plate) causes the magnetoelectric effect, resulting in the appearance of the non-diagonal terms with mixed polarizations. The Casimir force per unit area on the plates is obtained by differentiating Eq. (1) as $F(z) = -d\,E(z)/dz$. The existence of non-diagonal terms in the reflection matrices can lead to a change in the Casimir force not only in magnitude but also in its sign (changing from attractive to repulsive).

Furthermore, the dielectric function at imaginary frequencies $\varepsilon(i\xi)$ is vital to obtain the Casimir force between real materials using the Lifshitz theory. Since the precise optical characterization of materials was not used in the current analysis, we consider a broad variety of parameters for completeness assuming nonmagnetic TIs ($\mu = 1$). Due to the low concentration of free carriers in insulators, the proposed model[20,21] for the dielectric function at imaginary frequencies can be written as

$$\varepsilon(i\xi) = 1 + \frac{\omega_e^2}{\xi^2 + \omega_R^2 + \gamma_R\xi}. \quad (2)$$

This is considered the one oscillator model with resonant frequency ω_R and oscillator strength ω_e.[20,21] The damping parameter is described by γ_R, which is negligible in comparison with ω_R ($\gamma_R \ll \omega_R$).[20,21] In the first part of our analysis and discussion, we used $\omega_e/\omega_R = 0.6$, while in later sections, other values were used to investigate the dielectric effect, and applying a thin magnetic layer (of thickness $\ll$d with d being the separation between the plates) on the surface of the plates makes the TI layers fully insulating that allows their description by a dielectric function as in Refs. 20, 21, and 25. Moreover, the magnetic layer, which is considered a time reversal perturbation, is assumed thin enough to neglect any effect on the Casimir force. This situation can be controlled experimentally, and it can be defined by $\theta(\tilde{n}) = \tilde{n}\pi$, with $\tilde{n}$ being an odd integer value and $\theta(\tilde{n})$ being the so-called topological magnetoelectric polarizability (TEMP). The latter originates from the magnetoelectric effect modifying Maxwell's equations and, as a result, the electromagnetic Casimir force. Some estimations of the magnetic force contributions are given in Ref. 21 that make it feasible to probe the repulsion at 100 nm separations. In fact, the magnetic dipole–dipole interaction is of the order of attoN at distances of 50 nm and the magnetic Casimir force is 1 fN and much smaller than the expected Casimir forces of the order of 10–100 pN in agreement with recent measurements in TIs.[26] Thus, it is possible to neglect the magnetic interactions and take into consideration only the Casimir force experienced by the plates.

Besides the magnitude of the Casimir force, its nature (attractive or repulsive) is also sensitive to the magnetoelectric effect, and its tuning opens up new possibilities for devices. As it can be seen from Fig. 1(a), in the limit of short distances between the plates the positive values of $\tilde{\theta}$ (> 0) lead to an attractive Casimir force, while the repulsive force can be obtained for negative values of $\tilde{\theta}$ (< 0).[20,21] Notably, $\tilde{\theta} = \theta_1\,\theta_2$, where θ_1 and θ_2 belong to the first and second plates, respectively.[20,21] Using the Lifshitz theory, the attractive Casimir force between the two topological insulator plates with $\tilde{\theta} > 0$ (the same direction of the plate magnetizations) is given by

$$F(z) = \frac{\hbar}{2\pi^2}\int_0^\infty d\xi \int_0^\infty dk_\perp k_\perp k_0 \left\{\frac{\exp(-2k_0z)(2r_{sp}^2 + r_s^2 + r_p^2) - 2\exp(-4k_0z)[r_{sp}^2 - r_sr_p]^2}{1 + \exp(-4k_0z)(r_{sp}^2 - r_sr_p)^2 - (r_{sp}^2 + r_s^2 + r_p^2)\exp(-4k_0z)}\right\}, \quad (3)$$

while for $\tilde{\theta} < 0$ (opposite direction of the plate magnetization), the repulsive Casimir force is given by

$$F(z) = \frac{\hbar}{2\pi^2}\int_0^\infty d\xi \int_0^\infty dk_\perp k_\perp k_0 \left\{\frac{-\exp(-2k_0z)(2r_{sp}^2 - r_s^2 - r_p^2) - 2\exp(-4k_0z)[r_{sp}^2 - r_s\,r_p]^2}{1 + \exp(-4k_0z)(r_{sp}^2 - r_sr_p)^2 + (r_{sp}^2 - r_s^2 - r_p^2)\exp(-2k_0z)}\right\}. \quad (4)$$

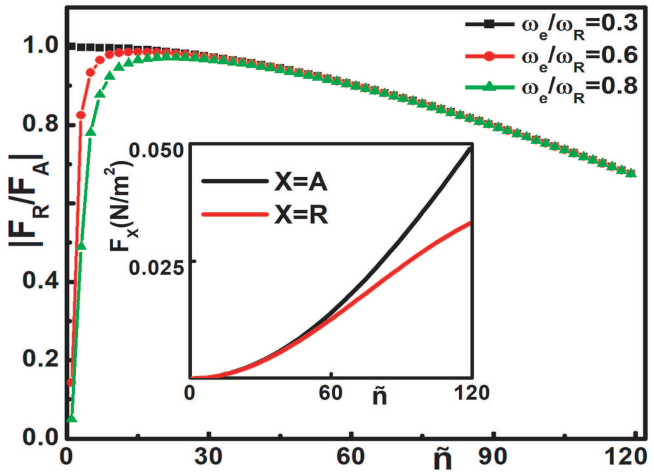

FIG. 3. The ratio of the repulsive to the attractive Casimir force (F_R/F_A) vs a wide range of the parameters for the TI dielectric function ($\omega_e/\omega_R = 0.3$ and 0.6 and 0.8). The separation between the plates is 250 nm. The inset shows the change of the attractive and repulsive forces vs magnetization for $\omega_e/\omega_R = 0.6$.

B. Actuation dynamics of MEM system

As a model actuating device, we considered a typical microswitch that consists of a fixed and a moving plate that is covered by TI materials and a thin magnetic layer (Fig. 1). The initial distance between the plates is assumed to be d = 500 nm. The moving plate is suspended by a mechanical spring, which is governed by Hooke's law.[27] The elastic restoring force $F_{res} = -k(d-z)$, where k is the stiffness of the spring, is the counterbalance of the Casimir force. The equation of motion for the system can be written as

$$M\frac{d^2z}{dt^2} + \left(\frac{M\omega_0}{Q}\right)\frac{dz}{dt} = -F_{res} + F_{Cas}, \tag{5}$$

where M is the mass of the moving plate, and $(M\omega_0/Q)(dz/dt)$ is the intrinsic energy dissipation of the moving plate with Q being the quality factor of the actuating system. In this study, we are considering high quality factors $Q \geq 10^4$ so that the effect of this term can be neglected.[28] Finally, we assumed actuating systems with resonance frequency $\omega_0 = 300$ kHz, which is typical for AFM cantilevers or MEMS.[5,28]

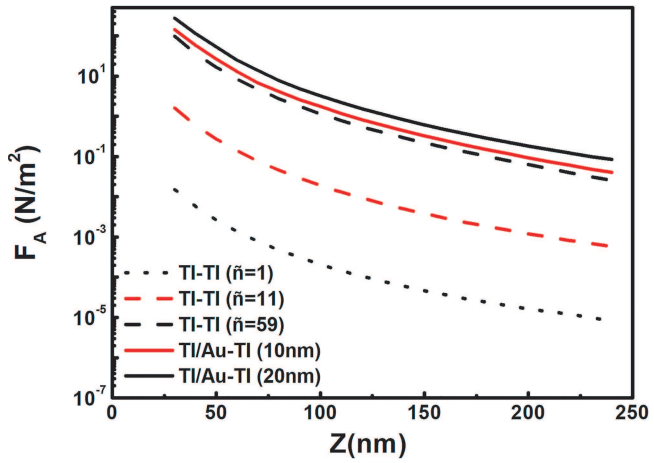

FIG. 4. Magnitude change of the Casimir force vs distance for the system TI–Au/TI, where the thin layer of Au has different thickness as indicated and for different magnetizations.

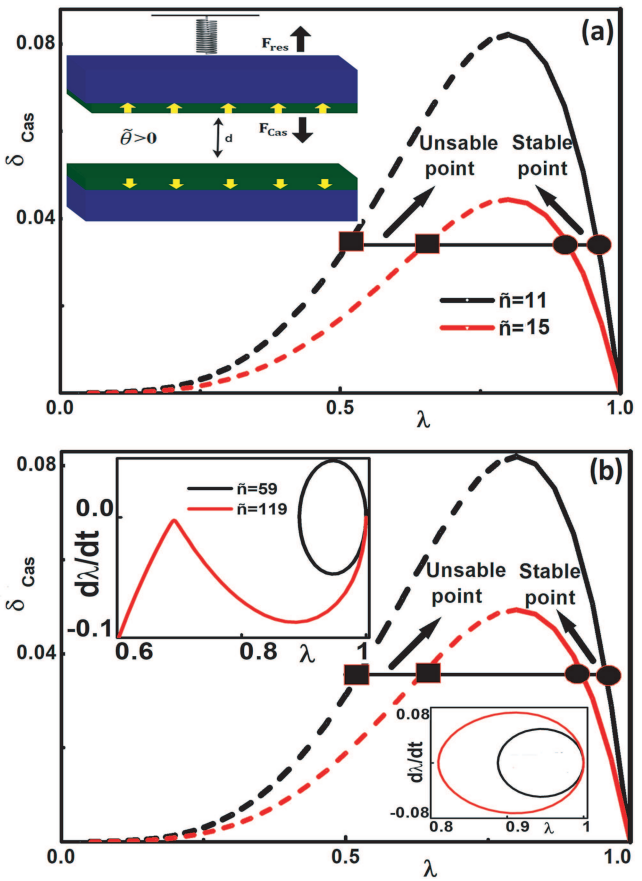

FIG. 5. Bifurcation diagrams δ_{Cas} vs $\lambda(= z/d)$ for (a) an intermediate magnitude magnetization, and (b) a strong magnitude of the magnetization having the same direction for both plates leading to attractive Casimir forces. The solid and dashed lines represent the stable and unstable points, respectively. The inset in (a) show the schematics of an actuating system. The insets in (b) show phase portraits for system with attractive Casimir forces respectively. δ_{Cas} are 0.042 (upper inset) and 0.033 (lower inset). Closed orbits describe stable motion, while open orbits describe unstable motion, which leads to stiction.

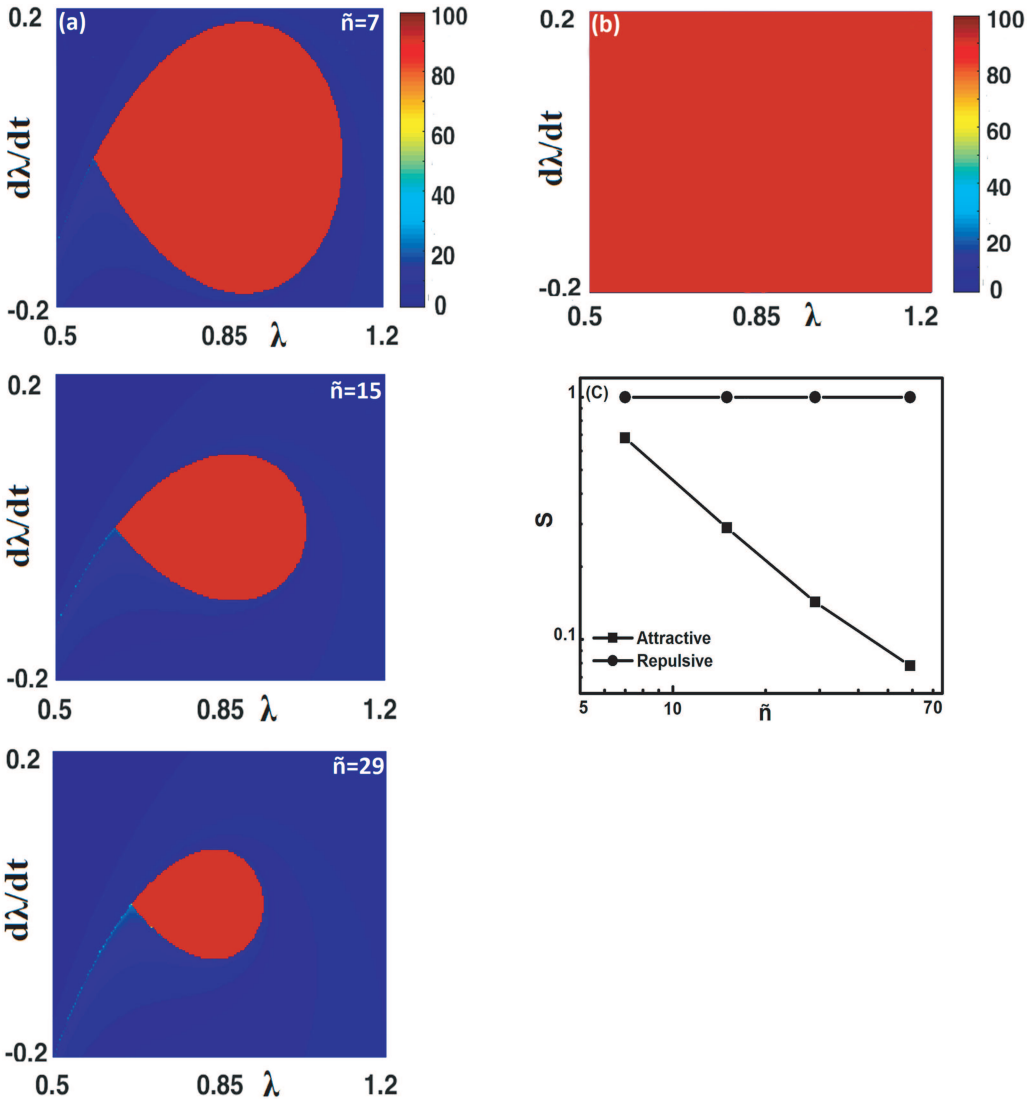

FIG. 6. Poincaré plots $d\lambda/dt$ vs λ. For the calculations, we used 200×200 initial conditions (λ, $d\lambda/dt$), $\delta_{Cas} = 0.04$, and $d = 350$ nm for both (a) attractive and (b) a repulsive Casimir forces. The magnitude of the magnetization is indicated for the case of attractive forces. The elliptical in shape homoclinic orbit contains the initial conditions that lead to stable oscillations. (c) The area of stable motion S [which has been normalized compared to repulsive forces in (b)] vs magnetization $\tilde{n}$ for both attractive and repulsive forces.

III. RESULTS AND DISCUSSION

A. Repulsive and attractive Casimir force between TI plates

Independent of the direction of the plate magnetizations, the magnitude of the Casimir force is amplified by an increase in the value of θ. The attractive force is stronger than the repulsive force in the weak and strong magnetization regimes, as it is shown in Fig. 1. It becomes more significant as magnetization and thus the magnetoelectric effect are weak. Furthermore, as the separation between the plates approaches small values, the force ratio becomes larger for these magnetization regimes. It can be claimed that at these distances, the magnetoelectric effect becomes more important resulting in an increased contribution of the off-diagonal terms in the reflection matrix and consequently, on the repulsive force.[20,21] In addition, the magnitude of repulsive force approaches zero as the separation between plates increases for systems with low magnetization due to the weaker contribution of the off-diagonal terms in the reflection matrix. Figure 1 also shows that a strong magnetoelectric effect leads to a long range repulsion force. This is the reason that

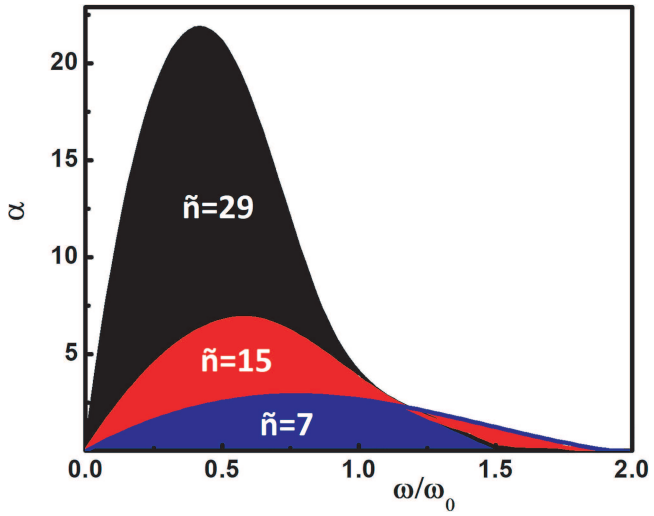

FIG. 7. Threshold curve $\alpha(=\sigma\omega_0 d/F_0)$ vs driving frequency ω/ω_o (with ω_o the natural frequency of the system) to compare the influence of the magnitude of the magnetization in the presence of attractive forces. It is considered $\delta_{Cas} = 0.04$ and the initial distance d = 350 nm.

this study is dedicated to the regime of short distances, where both attractive and repulsive forces are comparable for all values of the film magnetizations.

Figure 2 shows results for different values of the magnetization ($\tilde{n}$) of both plates. The magnetizations are initially in the same direction ($\tilde{\theta} > 0$), and then the direction of magnetization on one of the plates is reversed ($\tilde{\theta} < 0$), resulting in a repulsive Casimir force between the plates. The attractive force is stronger in the weak magnetization regime (small values of $\tilde{n}$) corresponding to the weak magnetoelectric effect. By increasing the magnetization ($\tilde{n}$), the system manifests with equal strength for both repulsive and attractive forces. To illustrate this, it can be stated that under this condition the magnetoelectric effect is strong enough ($|r_{sp}| >> |r_s|, |r_p|$) to determine both the direction (sign of $\tilde{\theta}$) and magnitude (strength of $\tilde{\theta}$) of the Casimir force. If the magnetization is increased further, the magnitude of the attractive force increases due to the increasing values of the Fresnel coefficients $|r_s|$ and $|r_p|$.

Furthermore, Fig. 3 quantifies how the ratio and magnitude (inset) of the repulsive to attractive forces varies as a function of the applied magnetizations $\tilde{n}$. In fact, the ratio increases until it reaches a peak, and after that it begins to decrease with increasing $\tilde{n}$. This figure shows that there is a maximum amount of repulsive force that can be produced when a certain value of the magnetization is applied. The aim in Fig. 3 is to compare the repulsive and attractive Casimir forces by taking into account the different dielectric functions besides the magnetizations. Due to the strong magnetoelectric effect, the ratio between the repulsive and attractive forces does not depend on the magnitude of the dielectric function in the range of strong magnetizations. However, for weak magnetization the reverse occurs, where by increasing the dielectric function (and thus r_s and r_p) the attractive force becomes stronger leading to a decreasing force ratio.

Finally, before proceeding to the analysis of the dynamic actuation, it is interesting to investigate the influence of a thin metal film on the Casimir force between the TI plates since the deposition of magnetic metal films on the TIs is essential to gap the surface states toward repulsive forces.[17–21] Figure 4 shows the Casimir force between two trivial TI plates in the presence of a thin layer of Au (since we have measured optical data for this material) on one of the plates. The metallic thin film yields a significant increase on the force since it is comparable to force between two non-trivial TI plates with strong magnetization in the same direction. Therefore, this figure clearly indicates that in a real system the effect of the metal film thickness must be taken into account also for the magnetic metallic films (which preferably must be less than 20 nm in thickness) in order to reduce shadowing of the TI–TI interactions.

B. Dynamic stability analysis

Our aim is to explore the area of stable operation of devices when the plate magnetizations are in the same or opposite direction leading, respectively, to attractive or repulsive Casimir forces. Therefore, we introduced the bifurcation parameter $\delta_{Cas} = F_{Cas}^{(m)}/F_{res}^{(M)}$ that represents the ratio of the minimum Casimir force to the maximum restoring force ($F_{res}^{(M)} = -kd$).[29] In terms of δ_{Cas}, Eq. (5) can be rewritten as

$$\frac{d^2\lambda}{dT^2} = -(1-\lambda) + \delta_{Cas}\frac{F_{Cas}}{F_{Cas}^{(m)}}, \tag{6}$$

where $\lambda = z/d$ and $T = \omega_0 t$. The equilibrium points of the actuating system can be obtained by setting the right part of Eq. (6) equal to zero. As a result, we obtain $\delta_{Cas} = (1-\lambda)(F_{Cas}^{(m)}/F_{Cas})$ for the case of attractive Casimir forces. When $\delta_{Cas} < 0$, as is the case of repulsive forces, then there are no equilibrium points and the system remains always under stable operation. In fact, according to Fig. 1, in this case, both the restoring and Casimir forces are synergistic, enabling stable operation for any initial conditions. Therefore, the bifurcation analysis will be devoted only to the case of attractive Casimir forces, where only limited stability is possible.

Figure 5 shows plots of δ_{Cas} vs λ for attractive Casimir forces assuming magnetizations of both intermediate and strong magnitude. As the plots show the maximum of δ_{Cas} decreases for a system with stronger magnetization. According to the bifurcation diagrams, if the restoring force is strong enough ($\delta_{Cas} < \delta_{Cas}^{(MAX)}$), then two equilibrium points exist. The stationary points located near $\lambda = 1$ describe stable centers for which periodic solutions exist. The other ones near to $\lambda = 0$ correspond to unstable points for which the system can no longer preserve its stability during oscillation around them due to the attractive Casimir force leading to stiction. Figure 5 shows the sensitivity of the bifurcation parameter to changes in magnetization. The region of stable operation is significantly wider for systems with small magnetization. Clearly, there are regions where the system with stronger magnetization loses its stable operation, while there are still equilibrium points for systems with smaller magnetization.

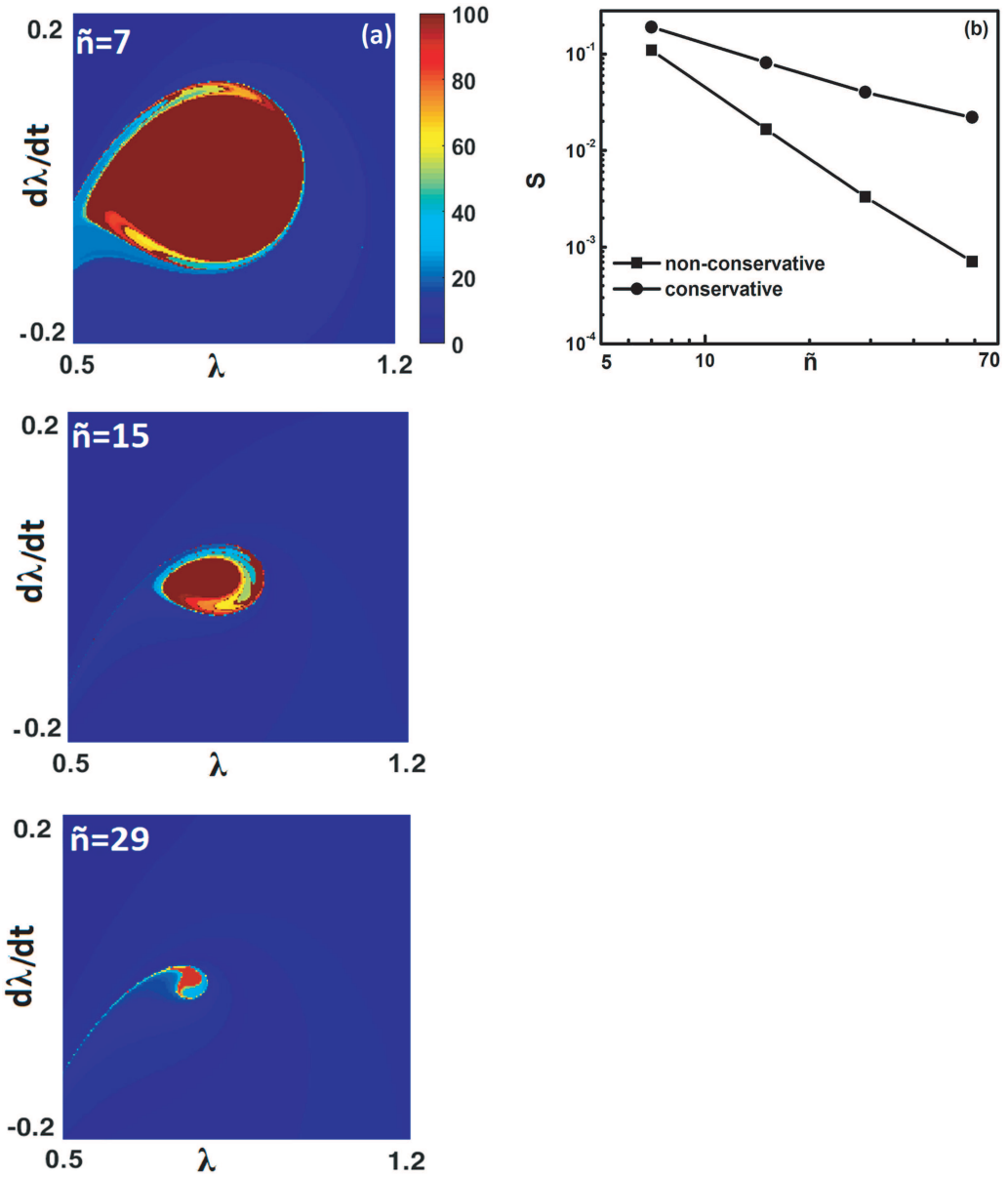

FIG. 8. (a) Poincaré plots of the transient times to stiction dλ/dt vs λ for the non-conservative system by applying magnetization on the same direction. The magnitude of the magnetizations is indicated. For computation, we used 200 × 200 initial conditions (λ, dλ/dt). We have considered $\alpha = 0.5$, $\omega/\omega_0 = 0.55$, $\delta_{Cas} = 0.04$, and d = 350 nm. (b) The area of stable motion S vs magnetization $\tilde{n}$ that is applied in same direction on the surfaces for both conservative and non-conservative oscillating devices.

Besides the bifurcation analysis, further information about the dynamics of the MEM system is obtained by the so-called phase portraits (d λ/dt vs λ).[30] The phase portraits for the attractive MEM system with different magnetizations are presented in the insets of Fig. 5(b). The closed orbits, which describe periodic movement around the stable center point, reveal strong sensitivity to changes of the magnetization. By increasing the magnetization, the orbit becomes larger due to the stronger Casimir force and consequently, requires a stronger restoring force to sustain stable operation. By increasing further the Casimir force and consequently δ_{Cas}, the periodic orbit turns into an unstable open orbit with the system losing its stability toward stiction.

Furthermore, the Poincaré maps in Fig. 6 demonstrate the regime of stable operation of the devices after 100 oscillations under

the presence of both attractive and repulsive Casmir forces by applying different magnetizations. It is clear that for the attractive Casimir forces, the increment of the magnetization will result in a strong reduction of the area of the homoclinic orbit that encloses all the stable periodic orbits, while for the repulsive Casimir force, the stable operation is always achieved independent of the magnetization. These points are reflected in Fig. 6(c), which shows quantitatively the drastic change in the stable operating area by comparing attractive and repulsive forces. In fact, fitting the data of the homoclinic area S for the case of attractive forces indicates a relatively inverse fast decay vs increasing magnetization as $S \sim \tilde{n}^{-1}$.

Finally, we will also present a brief study of the actuating device using as a perturbation term a small external applied periodic force $F_0 \cos(\omega\ t)$, as in Refs. 30 and 31, in order to investigate possible chaotic behavior. The equation of motion is given in this case by

$$M\frac{d^2z}{dt^2} + \left(\frac{M\omega_0}{Q}\right)\frac{dz}{dt} = -F_{res} + F_{Cas} + F_0\cos(\omega\ t). \tag{7}$$

The motion here is supposed to occur in clean and dry conditions in order to ignore capillary and hydrodynamic forces. Therefore, the source of the chaotic motion will be the splitting of the separatrix of the conservative system, which by the Smale–Birkhoff homoclinic theorem[32] yields the occurrence of chaotic motion. In the first-order approximation of the non-conservative system, the so-called Melnikov function can provide a solution for the splitting of the separatrix.[32] As a first-order perturbation on a conservative system, the Melnikov function is given by

$$M(T_0) = \frac{1}{Q}\int_{-\infty}^{+\infty}\left(\frac{d\varphi^C_{hom}(T)}{dT}\right)^2 dT + \frac{F_0}{F^{MAX}_{res}}\int_{-\infty}^{+\infty}\frac{d\varphi^C_{hom}(T)}{dT} \times \cos\left[\frac{\omega}{\omega_0}(T+T_0)\right]dT, \tag{8}$$

where $\varphi^C_{hom}(T)$ is the homoclinic solution of the conservative system. The separatrix splits if the Melnikov function has simple zeros so that $M(T_0) = 0$ and $M'(T_0) \neq 0$. If $M(T_0)$ has no zeros, the motion will not be chaotic. The conditions of nonsimple zeros, $M(T_0) = 0$ and $M'(T_0) = 0$ give the threshold condition for chaotic motion.[30,31] If we define

$$\mu^c_{hom} = \int_{-\infty}^{+\infty}\left(\frac{d\varphi^C_{hom}(T)}{dT}\right)^2 dT \text{ and } \beta(\omega) = \left|H\left[Re\left(F\left\{\frac{d\varphi^C_{hom}(T)}{dT}\right\}\right)\right]\right|, \tag{9}$$

then the threshold condition for chaotic motion $\alpha = \beta(\omega)/\mu^c_{hom}$ with $\alpha = (1/Q)(F_0/F^{MAX}_{res})^{-1} = \sigma\omega_0 d/F_0$ obtains the form

$$\alpha = \frac{\sigma\omega_{0\,d}}{F_0} = \left|H\left[Re\left(F\left\{\frac{d\varphi^C_{hom}(T)}{dT}\right\}\right)\right]\right| \Big/ \int_{-\infty}^{+\infty} \times \left(\frac{d\varphi^C_{hom}(T)}{dT}\right)^2 dT, \tag{10}$$

with $\sigma = M\omega_o/Q$ and $H[\cdots]$ denoting the Hilbert transform.[30,31]

Figure 7 shows the threshold curves α vs the driving frequency ratio ω/ω_o. For the area above the curve, where the magnitude of α is significant, the influence of the driving force is negligible as compared to dissipation since $\alpha \sim \sigma/F_0$. As a result, the motion approaches toward the stable periodic orbit of the conservative system. While below the curve, where the magnitude of α is smaller, the separatrix starts to split leading possibly to chaotic motion. Clearly, for the system with magnetizations in the same direction, the increment of the magnetization leads to the increment of the area below the threshold curve reflecting the increment of the attractive Casimir force and thus, the possibility for chaotic motion leading to stiction.

The occurrence of chaotic motion in terms of the sensitive dependence of the motion on its initial conditions is depicted by the Poincaré portraits in Fig. 8(a). The plots demonstrate that the motion can be chaotic after several periods prohibiting the long-term prediction of the actuation state for the device. This is because chaotic behavior introduces a significant risk for stiction, and this is more likely to take place when the attractive Casimir force increases, as it is the case with increasing magnetization (see Fig. 3, inset). According to Fig. 8(b), by increasing the magnetization in the same direction, which leads to increased attractive Casimir forces, the area of stable motion undergoes a remarkable rapid shrinkage for the periodically driven system. Indeed, this area follows an inverse power-law dependence $S \sim 1/\sim n^{2.8}$ as a function of the magnetization $\sim n$, while this effect is significantly weaker for the corresponding conservative system where the area under the homoclinic orbit decays as $S \sim 1/\sim n$.

IV. CONCLUSIONS

In conclusion, we have investigated the dynamical actuation of micro-electromechanical systems under the influence of attractive and repulsive Casimir forces between topological insulator plates as a function of their dielectric function and coating magnetization. The analysis of the Casimir force in the limit of strong and weak magnetization shows that the attractive force, which is produced for plate magnetizations in the same direction, is greater than the repulsive force that is produced for opposite magnetizations. However, both forces remain comparable for intermediate magnetizations. Moreover, for weak magnetization, the attractive force becomes stronger for an increasing dielectric function, while the opposite occurs for the repulsive force. On the other hand, increasing the magnetization decreases the influence of the dielectric function on both the repulsive and attractive forces. Furthermore, for conservative systems, bifurcation and phase portrait analysis revealed that an increasing magnetization decreases the regime of stable operation for devices with attractive forces, while their operation always remains stable under the presence of repulsive forces. Finally, for non-conservative periodically driven systems the Melnikov function and Poincaré portrait analysis show that magnetizations in the same direction lead to strong attractive Casimir forces and consequently chaos. Chaotic motion toward stiction is highly likely to occur preventing the long term prediction of actuating dynamics. A remedy for this situation is obtained by the application of any magnetization in opposite directions between the interacting surfaces since the repulsive force makes it possible to prevent stiction. It should be stressed that for a system operating in ambient

conditions, though in the present study, we focused on systems operating in vacuum, other attractive forces (e.g., capillary forces) must be carefully accounted for complete analysis of the effect of repulsive Casimir forces and their potency to prevent stiction under any environmental conditions.

ACKNOWLEDGMENTS

G.P. acknowledges support from the Zernike Institute for Advanced Materials at University of Groningen. A.A.M. and F.T. acknowledge the support from the Department of Physics at Alzahra University.

APPENDIX A: THE LIFSHITZ THEORY FOR STRATIFIED MEDIA AND DIELECTRIC FUNCTION OF MATERIALS WITH EXTRAPOLATIONS

The reflection matrices $R_{1,2}$ are 2×2 and consist of the Fresnel coefficients. The latter are derived from Maxwell's equations by imposing the continuity relations for the normal components of the electromagnetic field. The Fresnel reflection coefficients are defined by r_s and r_p and $r_{sp,}$ which show transverse electric (TE) and magnetic (TM) fields and mixed (TEM) polarizations, respectively. r_s and r_p are the diagonal terms, and r_{sp} is placed as non-diagonal terms. In the case of a trivial topological insulator (without a magnetic layer), the reflection matric becomes diagonal and can be represented as

$$R_1 = \begin{bmatrix} r_s^1 & 0 \\ 0 & r_p^1 \end{bmatrix}, \quad R_2 = \begin{bmatrix} r_s^2 & 0 \\ 0 & r_p^2 \end{bmatrix}. \tag{A1}$$

In Eq. (A1), R_1 and R_2 are the reflection matrices for the first and second plates, respectively. Using the Lifshitz theory, the Casimir force ($F_{Cas}(z)$) at $T = 0$ k is given by[4]

$$F_{Cas}(z) = \frac{\hbar}{2\pi^2} \int_0^\infty d \sum\nolimits_{\nu=s,s} \int_0^\infty dk_\perp k_\perp k_0 \frac{r_\nu^{(1)} r_\nu^{(2)} exp(-2k_0 z)}{1 - r_\nu^{(1)} r_\nu^{(2)} exp(-2k_0 z)}. \tag{A2}$$

The imaginary frequencies are shown by ξ and $k_i = \sqrt{\varepsilon_i(i\xi_l)\xi^2/c^2 + k_\perp^2}$, where $(i = 0, 1, 2)$ represents the out-off plane wave vector in the gap between the interacting plates (k_0) and in each of the interacting plates ($k_{i=(1,2)}$). $k_\perp$ is the in-plane wave vector.

When we are considering a thin magnetic layer on the surface of the plates, the non-diagonal terms appear in the reflection matrices due to the magnetoelectric effect and consequently, the matrices can be written as

$$R_1 = \begin{bmatrix} r_s^1 & r_{sp}^1 \\ r_{sp}^1 & r_p^1 \end{bmatrix} \quad R_2 = \begin{bmatrix} r_s^2 & +/- r_{sp}^2 \\ +/- r_{sp}^2 & r_p^2 \end{bmatrix}, \tag{A3}$$

where $+r_{Sp}^2$ describes the same direction of the magnetizations on the surface and plates, while the opposite direction of the magnetization on the surface and plates is defined by $-r_{Sp}^2$. The reflection coefficients can be written as

$$r_s^i = \frac{(k_0 - k_i)(\varepsilon k_0 + k_i) - k_i\, k_0 \tilde{\alpha}_i^2}{(k_0 + k_i)(\varepsilon k_0 + k_i) + k_i\, k_0 \tilde{\alpha}_i^2}, \tag{A4}$$

$$r_p^i = \frac{(k_0 + k_i)(\varepsilon k_0 - k_i) - k_i\, k_0 \tilde{\alpha}_i^2}{(k_0 + k_i)(\varepsilon k_0 + k_i) + k_i\, k_0 \tilde{\alpha}_i^2}, \tag{A5}$$

$$r_{sp}^i = \frac{2k_i k_0 \tilde{\alpha}_i^2}{(k_0 + k_i)(\varepsilon k_0 + k_i) + k_i\, k_0 \tilde{\alpha}_i^2}, \tag{A6}$$

where $\tilde{\alpha}_i = \alpha\theta_i/\pi$ and $\alpha = 1/137$ is the fine structure constant. According to Eqs. (1) and (A3), the Casimir force between two topological insulators with the same and opposite directions of magnetization has been calculated using Eqs. (3) and (4).

AUTHOR DECLARATIONS

Conflict of Interest

The authors have no conflicts to disclose.

Author Contributions

F. Tajik: Conceptualization (equal); Formal analysis (equal); Investigation (equal); Methodology (equal); Supervision (equal); Writing – original draft (equal). **N. Allameh:** Investigation (equal); Writing – original draft (equal). **A. A. Masoudi:** Supervision (equal); Writing – original draft (equal). **G. Palasantzas:** Conceptualization (equal); Supervision (equal); Writing – review & editing (equal).

DATA AVAILABILITY

The data that support the findings of this study are available from the corresponding author upon reasonable request.

REFERENCES

[1] H. B. G. Casimir, "Zero point energy effects on quantum electrodynamics," Proc. K. Ned. Akad. Wet. **51**, 793 (1948).
[2] A. W. Rodriguez, F. Capasso, and S. G. Johnson, "The Casimir effect in microstructured geometries," Nat. Photonics **5**, 211 (2011).
[3] F. Capasso, J. N. Munday, D. Iannuzzi, and H. B. Chan, "Casimir forces and quantum electrodynamical torques: Physics and nanomechanics," IEEE J. Sel. Top. Quantum Electron. **13**, 400 (2007).
[4] M. Bordag, G. L. Klimchitskaya, U. Mohideen, and V. M. Mostepanenko, *Advances in the Casimir Effect* (Oxford University Press, New York, 2009).
[5] R. S. Decca, D. Łopez, E. Fischbach, G. L. Klimchitskaya, D. E. Krause, and V. M. Mostepanenko, "Precise comparison of theory and new experiment for the Casimir force leads to stronger constraints on thermal quantum effects and long-range interactions," Ann. Phys. (NY) **318**, 37 (2005); M. Bordag, G. L. Klimchitskaya, U. Mohideen, and V. M. Mostepanenko, "Tests of new physics from precise measurements of the Casimir pressure between two gold-coated plates," Phys. Rev. D **75**, 077101 (2007).
[6] E. M. Lifshitz, "The theory of molecular attractive forces between solids," in *Perspectives in Theoretical Physics: The Collected Papers of E. M. Lifshitz*, edited by L. P. Pitaevski (Pergamon, 1992), pp. 329–349; I. E. Dzyaloshinskii, E. M. Lifshitz, and L. P. Pitaevskii, "General theory of van der Waals forces," Sov. Phys. Usp. **4**, 153 (1961).
[7] P. Ball, "Fundamental physics: Feel the force," Nature **447**, 772 (2007).
[8] H. G. Craighead, "Nanoelectromechanical systems," Science **290**, 1532 (2000).

[9]F. Tajik, M. Sedighi, Z. Babamahdi, A. A. Masoudi, H. Waalkens, and G. Palasantzas, "Dependence of non-equilibrium Casimir forces on material optical properties towards chaotic motion during device actuation," Chaos **29**, 093126 (2019).
[10]F. Tajik, A. A. Masoudi, Z. Babamahdi, M. Sedighi, and G. Palasantzas, "Sensitivity of non-equilibrium Casimir forces on low frequency optical properties towards chaotic motion of microsystems," Chaos **30**, 023108 (2020).
[11]F. Tajik, M. Sedighi, M. Khorrami, A. A. Masoudi, and G. Palasantzas, "Chaotic behavior in Casimir oscillators: A case study for phase-change materials," Phys. Rev. E **96**, 042215 (2017); F. Tajik, M. Sedighi, and G. Palasantzas, "Sensitivity on materials optical properties of single beam torsional Casimir actuation," J. Appl. Phys. **121**, 174302 (2017).
[12]F. Tajik, M. Sedighi, M. Khorrami, A. A. Masoudi, H. Waalkens, and G. Palasantzas, "Dependence of chaotic behavior on optical properties and electrostatic effects in double-beam torsional Casimir actuation," Phys. Rev. E **98**, 02210 (2018).
[13]M. Sedighi and G. Palasantzas, "Casimir and hydrodynamic force influence on microelectromechanical system actuation in ambient conditions," Appl. Phys. Lett. **104**, 074108 (2014).
[14]M. Sedighi, V. B. Svetovoy, W. H. Broer, and G. Palasantzas, "Casimir forces from conductive silicon carbide surfaces," Phys. Rev. B **89**, 195440 (2014); M. Sedighi, F. Tajik, S. M. Mahmoudi, M. H. Nazarpak, G. R. R. Lamouki, G. Palasantzas, "Sensitivity of Casimir oscillator on geometry and optical properties," Mod. Phys. Lett. A, **35**, 2040003 (2020).
[15]F. M. Serry, D. Walliser, and G. J. Maclay, "The role of the Casimir effect in the static deflection and stiction of membrane strips in microelectromechanical systems (MEMS)," J. Appl. Phys. **84**, 2501 (1998); F. M. Serry, D. Walliser, and G. J. Maclay, "The role of the Casimir effect in the static deflection and stiction of membrane strips in microelectromechanical systems (MEMS)," J. Microelectromech. Syst. **4**, 193 (1995); G. Palasantzas and J. T. M. DeHosson, "Phase maps of microelectromechanical switches in the presence of electrostatic and Casimir forces," Phys. Rev. B **72**, 121409 (2005); G. Palasantzas and J. T. M. DeHosson, "Pull-in characteristics of electromechanical switches in the presence of Casimir forces: Influence of self-affine surface roughness," Phys. Rev. B **72**, 115426 (2005).
[16]F. W. DelRio, M. P. de Boer, J. A. Knapp, E. D. Reedy, Jr., P. J. Clews, and M. L. Dunn, "The role of van der Waals forces in adhesion of micromachined surfaces," Nat. Mater. **4**, 629 (2005).
[17]M. Z. Hasan and C. L. Kane, "Topological insulators," Rev. Mod. Phys. **82**, 3045 (2010).
[18]J. E. Moore, "The birth of topological insulators," Nature (London) **464**, 194 (2010).
[19]D. Hsieh, D. Qian, L. Wray, Y. Xia, Y. Hor, R. J. Cava, and M. Hasan, "Topological Dirac insulator in a quantum spin Hall phase," Nature (London) **452**, 970 (2008).
[20]A. G. Grushin and A. Corteijo, "Tunable Casimir repulsion with three-dimension topological insulators," Phys. Rev. Lett **106**, 020403 (2011).
[21]A. G. Grushin, P. Rodriguez-Lopez, and A. Cortijo, "Effect of finite temperature and uniaxial anisotropy on the Casimir effect with three-dimensional topological insulators," Phys. Rev. B **84**, 045119 (2011).
[22]V. N. Marachevsky, Phys. Rev. B **99**, 075420 (2019); V. N. Marachevsky, "Casimir interaction of two dielectric half spaces with Chern-Simons boundary layers," Mod. Phys. Lett. A **35**, 2040015 (2020).
[23]I. Fialkovsky, N. Khusnutdinov, and D. Vassilevich, "Quest for Casimir repulsion between Chern-Simons surfaces," Phys. Rev. B **97**, 165432 (2018).
[24]L. M. Woods, D. A. R. Dalvit, A. Tkatchenko, P. Rodriguez-Lopez, A. W. Rodriguez, and R. Podgornik, "Materials perspective on Casimir and van der Waals interactions," Rev. Mod. Phys **88**, 045003 (2016); B. S. Lu, Universe **7**, 237 (2021).
[25]X. L. Qi, R. LI, J. Zang, and S. C. Zhang, "Inducing a magnetic monopole with topological surface states," Science **323**, 1184 (2009).
[26]Z. Babamahdi, V. B. Svetovoy, W. H. Broer, D. T. Yimam, B. J. Kooi, T. Banerjee, J. Moon, S. Oh, M. Enache, M. Stöhr, and G. Palasantzas, "Casimir and electrostatic forces from Bi_2Se_3 thin films of varying thickness," Phys. Rev. B Lett. **103**, L161102 (2021).
[27]J. A. Pelesko and D. H. Bernstein, *Modeling MEMS and NEMS* (Chapman & Hall/CRC, Boca Raton, FL, 2003).
[28]R. Garcıa and R. Perez, "Dynamic atomic force microscopy methods," Surf. Sci. Rep. **47**, 197 (2002); D. Rugar, R. Budakian, H. J. Mamin, and B. W. Chui, "Single spin detection by magnetic resonance force microscopy," Nature **430**, 329 (2004).
[29]S. Cui and Y. C. Soh, "An accurate separation estimation algorithm for the Casimir oscillator," J. Microelectromech. Syst. **19**, 1153 (2010).
[30]M. W. Hirsch, S. Smale, and R. L. Devaney, *Differential Equations, Dynamical Systems, and an Introduction to Chaos* (Elsevier Academic Press, San Diego, CA, 2004).
[31]W. Broer, H. Waalkens, V. B. Svetovoy, J. Knoester, and G. Palasantzas, "Nonlinear actuation dynamics of driven Casimir oscillators with rough surfaces," Phys. Rev. Appl. **4**, 054016 (2015).
[32]J. Guckenheimer and P. Holmes, *Nonlinear Oscillations, Dynamical Systems, and Bifurcations of Vector Fields* (Springer-Verlag, New York, 1986).